International Journal of Heat and Mass Transfer 53 (2010) 4238–4247

Contents lists available at ScienceDirect

International Journal of Heat and Mass Transfer

journal homepage: www.elsevier.com/locate/ijhmt

Constructal design of nanofluids

Jing Fan, Liqiu Wang *

Department of Mechanical Engineering, The University of Hong Kong, Pokfulam Road, Hong Kong

ARTICLE INFO

Article history:
Received 22 January 2010
Received in revised form 10 May 2010
Accepted 11 May 2010
Available online 11 June 2010

Keywords:
Constructal design
Inverse problem
Heat conduction
Optimization
Nanofluids

ABSTRACT

We develop a constructal approach that is capable of finding constructal microstructure of nanofluids for constructal system performance. The approach converts the inverse problem of optimizing the microstructure for the best system performance into a forward one by first specifying a type of microstructures and then optimizing system performance with respect to the available freedom within the specified type of microstructures. The approach is applied to constructal design of nanofluids with any branching level of tree-shaped nanostructures in a circular disc with uniform heat generation. The constructal configuration and constructal system thermal resistance have some elegant universal features for both cases of given aspect ratio of the periphery sectors and given the total number of slabs in the periphery sectors, respectively. While our focus is on the constructal design and optimization of nanofluids microstructure, the methodologies and results are equally valid for other problems such as heat conduction optimization for cooling a disc-shaped area.

1. Introduction

Nanofluids are the fluid suspensions of nanometer-sized structures (particles, fibers, tubes) [1–3]. Recent experiments on nanofluids have shown, for example, twofold increases in thermal conductivity [2,4,5], strong temperature dependence of thermal conductivity [3], substantial increases in convective heat transfer coefficient [3,6], and threefold increases in critical heat flux (CHF) in boiling heat transfer [1–3,7]. These characteristics make them very attractive for a large number of industries such as transportation, electronics, defense, space, nuclear systems cooling and biomedicine [1–3].

The very essence of nanofluids research and development is to enhance system overall performance through manipulating nanoparticles' structure and distribution in the base fluids. For the heat-conduction nanofluids, the desire for the system overall performance is normally to minimize system highest temperature or to minimize system overall thermal resistance. Therefore, interest should focus not only on improving nanofluid thermal conductivity but also on designing nanofluid structures for better system overall performance [8].

By its very nature, the optimization of nanofluid microstructures for better system performance fits well into the inverse problem in mathematics and the downscaling problem in multiscale science [9]. Both are of fundamental importance but daunting difficulty with no effective method available to resolve them at present. We thus propose a constructal approach that follows the constructal theory [10–12] and is capable of finding constructal microstructure and constructal performance. Here constructal microstructure and performance are the best microstructure and performance within a specified type of microstructures. In the present work, we show this approach by performing a constructal design for nanofluid heat conduction in a circular disc with the prespecified type of microstructures of tree configuration in which nanoparticles form tree structures in the base fluid as high-conductivity channels for the heat flow (Fig. 1). The tree structure is chosen because it is mostly found in nature for its small flow resistance [10–12].

The circular disc system is selected both for its fundamental importance and for its geometrical regularity that renders an analytical analysis possible. For addressing the fundamental issue in the cooling of electronics, this system was first studied in [13] by adopting the 'growth' method of constructal design [14]. The constructal design in [13] started with the optimization of the elemental sector (the smallest area sector) for the minimization of the sector thermal resistance. Such optimized elemental sectors were used to build the system. The constructal system structure was then obtained by minimizing the overall system thermal resistance with respect to the distribution of volume fraction of high-conductivity material. The resulted constructal overall resistance was shown to decrease with the dimensionless disc radius defined as the ratio of the disc radius over the square root of elemental sector area. As the disc size becomes larger and larger compared with the elemental sector, a structure with more branching levels would be recommended. The present work focuses on designing microstructure of the fixed-sized system for minimizing system overall thermal resistance. Therefore, neither the aspect ratio nor the size of

* Corresponding author.
E-mail address: lqwang@hku.hk (L. Wang).

0017-9310/$ - see front matter © 2010 Elsevier Ltd. All rights reserved.
doi:10.1016/j.ijheatmasstransfer.2010.05.050

Nomenclature

a_{M1} constant appearing in the constructal system thermal resistance of M-branching architecture for fixed aspect ratio of the periphery sectors
a_{M2} constant appearing in the constructal system thermal resistance of M-branching architecture for fixed number of slabs in the periphery sectors
b_{M1} constant constructal relative radius $\overline{R}_0$ of M-branching architecture for fixed aspect ratio of the periphery sectors
b_{M2} constant constructal relative radius $\overline{R}_0$ of M-branching architecture for fixed number of slabs in the periphery sectors
c_{M1} constant constructal slab volume fraction $\tilde{\varphi}_{1\sim M,con}$ for fixed aspect ratio of the periphery sectors
c_{M2} constant constructal slab volume fraction $\tilde{\varphi}_{1\sim M,con}$ for fixed number of slabs in the periphery sectors
D_i slab width in Level-i sectors (m)
$\widetilde{D}_{i,Mth}$ non-dimensional slab width in Level-i sectors of M-branching architecture, $D_i/(D_M\prod_{j=i+1}^{M}n_j)$
H_i half-base-length in Level-i sectors (m)
k Thermal conductivity ratio of nanoparticles and the base fluid, k_p/k_f
k_f thermal conductivity of the base fluid (W/(m K))
k_p thermal conductivity of nanoparticles (W/(m K))
L_i slab length in Level-i sectors (m)
n_i bifurcation number from one slab in the Level-i sectors
N_i total number of slabs in the Level-i sectors
r radial position (m)
R_0 radius of the whole disc (m)
$R_{i,Mth}$ distance from the confluence point of the slabs in Level-i sectors to the rim in M-branching architecture, $\sum_{j=i}^{M}L_j$ (m)
$\overline{R}_i$ non-dimensional relative radius of Level-i sectors, R_i/R_{i+1}
R_{Mth} disc overall thermal resistance in M-branching architecture
q''' volumetric heat generation rate (W/m^3)
T_0 center temperature (K)
T_c temperature at the confluence point in one-branching architecture (K)
T_{c1} temperature at the confluence point of the slabs in Level-1 sectors (K)
T_{c2} temperature at the confluence point of the slabs in Level-2 sectors (K)
T_m hot-spot temperature (K)
T_R temperature at the peripheral tip of slabs in zero-branching architecture (K)
α_0 angle of one central sector
φ overall slab volume fraction
φ_i slab volume fraction in Level-i sectors
$\varphi_{i\sim M}$ slab volume fraction from Level-i to Level-M
$\tilde{\varphi}_{i\sim M}$ Non-dimensional slab volume fraction, $\varphi_{i\sim M}/\varphi_{(i-1)\sim M}$

Subscripts
con constructal
ith Level-i sectors
Mth Level-M sectors

the elemental sector is fixed in our analysis because the employment of elemental sectors with a minimized sector resistance does not necessarily yield a minimization of system overall resistance. We introduce length ratios of sectors at different positions so that once the number of branching level is specified the constructal design provides directly the optimized length of each sector relative to the disc radius and the optimized distribution of volume fractions. Furthermore, our constructal design is made for configurations with any levels of tree branching.

The present work centers on obtaining the theoretically best tree structure rather than modeling or resembling the clustering/agglomerating in the real systems of nanofluids. The obtained constructal structure offers the direction (theoretically the best) for developing high-performance nanofluids. While our focus is on the constructal design and optimization of nanofluids microstructure, the methodologies are equally valid for other problems of constructal design such as surface-to-point heat conduction and constructal allocation of materials with different properties [10–15].

2. Constructal design

Consider nanofluid heat conduction in a circular disc of radius R_0 and unit thickness, with uniform distribution of volumetric heat generation rate q''' and one central heat sink (T_0) (Fig. 1). Nanoparticles are assumed to be thin slabs and form tree configuration in the base fluid as high-conductivity channels for the heat flow. The composition of the nanoparticles and the base fluid is fixed and specified by the particle volume fraction φ over the total nanofluid volume:

$$\varphi = \frac{\text{volume of nanoparticle material}}{\text{total nanofluid volume}}. \tag{1}$$

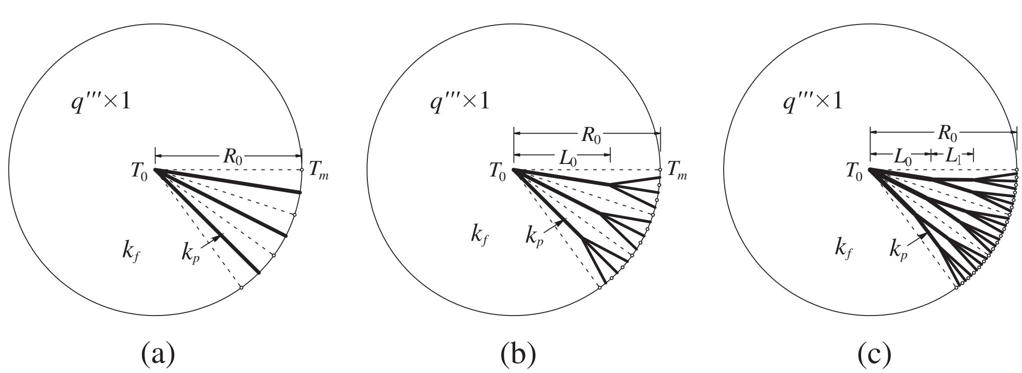

Fig. 1. Nanofluid heat conduction in a circular disc of radius R_0: (a) zero-branching architecture; (b) one-branching architecture; and (c) two-branching architecture.

Our goal is to optimize the geometry of the heat-conduction paths for minimizing the overall thermal resistance, that is, the hot-spot temperature T_m, which is likely to occur on the rim.

2.1. Zero-branching architecture

The simplest architecture is the one with no slab branching so that the slabs arranged radially and equidistantly with one end touching the heat sink and the other touching the rim as shown in Fig. 1(a) [10]. For the sake of simplicity, the following assumptions are made [8,10,13]:

(i) there are many radial slabs (with conductivity of k_p) so that one elemental sector is slender enough to be approximated by an isosceles triangle of base $2H_0$ and height R_0 [Fig. 2(a)];
(ii) the width D_0 of each slab is constant;
(iii) the volume fraction φ of the slabs is fixed and small, $\varphi \ll 1$;
(iv) the conductivity ratio between slabs and base fluid is fixed and large, $k = k_p/k_f \gg 1$.

Therefore, the freedom of the zero-branching architecture is the aspect ratio of the element, H_0/R_0. By following that in [8,10,13] for evaluating $(T_m - T_R)$ and $(T_R - T_0)$ under the above assumptions, we have the overall temperature difference and thermal resistance of the whole disc:

$$(T_m - T_0)_{0th} = \frac{q'''H_0^2}{2k_f} + \frac{2q'''R_0^2}{3k_p\varphi}, \tag{2}$$

$$R_{0th} = \frac{(T_m - T_0)_{0th}}{q'''\pi R_0^2/k_f} = \frac{(H_0/R_0)^2}{2\pi} + \frac{2}{3\pi k\varphi}. \tag{3}$$

Clearly, the system overall thermal resistance R_{0th} becomes smaller and approaches to $2/(3\pi k\varphi)$ as H_0/R_0 decreases.

2.2. One-branching architecture

One-branching architecture consists of slabs that stretch radially to the distance L_0 away from the central heat sink, and continue with n_1 branches that reach the rim [Fig. 1(b); 8, 10, 13]. Its elemental sector contains one stem of aspect ratio H_0/L_0 and n_1 tributaries of aspect ratio H_1/L_1 shown in Fig. 2(b). The length L_1 is the distance from the hot spot (T_m) to the confluence point (T_c). The goal is to assemble a number of branched sectors into a complete disc for a minimum overall thermal resistance.

The system overall temperature difference $(T_m - T_0)$ can be calculated by the sum of $(T_m - T_c)$ and $(T_c - T_0)$. By applying the result from zero-branching architecture [Eq. (2)], $(T_m - T_c)$ in the periphery sectors with radius of L_1 can be estimated by

$$T_m - T_c = \frac{q'''H_1^2}{2k_f} + \frac{2q'''L_1^2}{3k_p\varphi_1}. \tag{4}$$

Here φ_1 is the slab volume fraction in the periphery sector and equals to D_1/H_1 with D_1 as the slab width in the periphery sector.

The T_c tip of each slab receives the heat current collected by the n_1 periphery sectors, which equals to the heat generation in the area between the dashed arc with radius L_0 and the outer circumference. Therefore, an energy balance at the tip yields

$$q''' \times 1 \times \frac{\pi R_0^2 - \pi L_0^2}{(2\pi/\alpha_0)} = 1 \times k_p D_0 \left(\frac{dT}{dr}\right)_{r=L_0}. \tag{5}$$

Here α_0 is the angle of one central sector,

$$\alpha_0 = \frac{2n_1H_1}{R_0}. \tag{6}$$

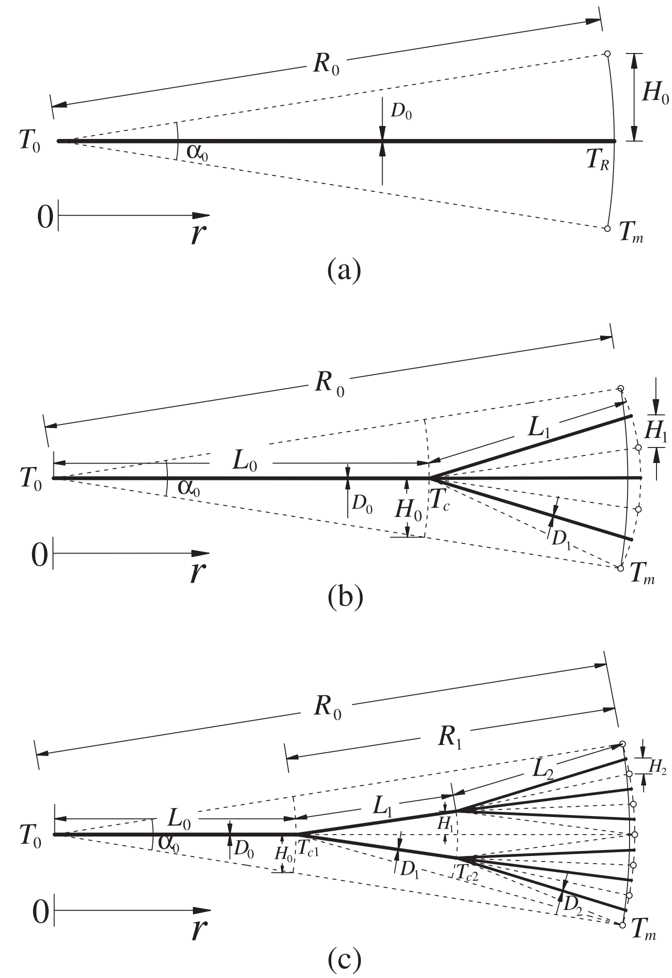

Fig. 2. Elemental sector of (a) zero-branching architecture, (b) one-branching architecture ($n_1 = 3$ for example) and (c) two-branching architecture ($n_1 = 2$, $n_2 = 3$ for example).

r is the radial position measured from the center ($r = 0$) to the T_c junction ($r = L_0$). The governing equation for the temperature distribution along the D_0 slab is [8,10,13]

$$-dq = 2\left(\frac{H_0}{L_0}r\right)q''' \times 1\,dr, \tag{7}$$

where

$$q = 1 \times k_pD_0\frac{dT}{dr}. \tag{8}$$

After invoking the tip condition, Eq. (5), a successive integration of Eqs. (7) and (8) leads to the temperature difference $(T_c - T_0)$

$$T_c - T_0 = \frac{q'''L_0}{k_pD_0}\left[\frac{2}{3}H_0L_0 + \frac{n_1H_1}{R_0}(R_0^2 - L_0^2)\right]. \tag{9}$$

Applying $L_0 \cong R_0 - L_1$, Eqs. (4) and (9) give the disc overall temperature difference:

$$(T_m - T_0)_{1th} = \frac{q'''H_1L_1}{k_f}\left(\frac{1}{2}\frac{H_1}{L_1} + \frac{2}{3k\varphi_1}\frac{L_1}{H_1}\right) + \frac{q'''L_0}{k_pD_0}\left[\frac{2}{3}H_0L_0 + \frac{n_1H_1}{R_0}(R_0^2 - L_0^2)\right]. \tag{10}$$

The disc overall thermal resistance can thus be written as

$$R_{1th}=\frac{(T_m-T_0)_{1th}}{q'''\pi R_0^2/k_f}=\frac{1}{\overline{R}_{0,1th}^2}\left\{\frac{(H_1/L_1)^2}{2\pi}+\frac{2}{3\pi k\varphi_1}\right\}+\frac{1}{\pi k\varphi_1}\frac{1}{\widetilde{D}_{0,1th}}\left(1-\frac{1}{\overline{R}_{0,1th}}\right)\left[1-\frac{1}{3}\left(1-\frac{1}{\overline{R}_{0,1th}}\right)^2\right], \tag{11}$$

where

$$\overline{R}_{0,1th}=\frac{R_0}{L_1},\quad \widetilde{D}_{0,1th}=\frac{D_0}{n_1D_1}. \tag{12}$$

The term in the braces {} is the same as the one obtained by replacing H_0/R_0 and φ in R_{0th} with H_1/L_1 and φ_1, respectively.

Since the overall particle volume fraction φ can be expressed as

$$\varphi=\frac{(n_1D_1L_1+D_0L_0)(2\pi/\alpha_0)}{\pi R_0^2}=\frac{n_1D_1L_1+D_0L_0}{n_1H_1R_0}, \tag{13}$$

we have

$$\widetilde{D}_{0,1th}=\frac{(\varphi/\varphi_1)\overline{R}_{0,1th}-1}{\overline{R}_{0,1th}-1},\quad \varphi_1<\varphi\overline{R}_{0,1th}. \tag{14}$$

Therefore, the system overall thermal resistance R_{1th} is a function of H_1/L_1, φ_1 and $\overline{R}_{0,1th}$. R_{1th} will have a minimum value when

$$\frac{\partial R_{1th}}{\partial(H_1/L_1)}=0, \tag{15}$$

$$\frac{\partial R_{1th}}{\partial\varphi_1}=0, \tag{16}$$

$$\frac{\partial R_{1th}}{\partial\overline{R}_{0,1th}}=0. \tag{17}$$

However,

$$\frac{\partial R_{1th}}{\partial(H_1/L_1)}=\frac{H_1/L_1}{\pi\overline{R}_{0,1th}^2}\geqslant 0. \tag{18}$$

Therefore, R_{1th} is monotonically decreases when (H_1/L_1) tends to zero for fixed φ_1 and $\overline{R}_{0,1th}$. To satisfy Eq. (16), we have

$$\frac{\partial}{\partial\varphi_1}\left\{\frac{a}{\overline{R}_{0,1th}^2\varphi_1}+\frac{\overline{R}_{0,1th}-1}{\varphi\overline{R}_{0,1th}-\varphi_1}\left(1-\frac{1}{\overline{R}_{0,1th}}\right)\left[1-\frac{1}{3}\left(1-\frac{1}{\overline{R}_{0,1th}}\right)^2\right]\right\}=0, \tag{19}$$

where $a = 2/3$. Its solution yields the constructal φ_1

$$\tilde{\varphi}_{1,con}=\varphi_{1,con}/\varphi=\frac{a\overline{R}_{0,1th}}{A_1}\left(\sqrt{1+\frac{A_1}{a}}-1\right), \tag{20}$$

where

$$A_1=(\overline{R}_{0,1th}-1)\left(1-\frac{1}{\overline{R}_{0,1th}}\right)\left[\overline{R}_{0,1th}^2-\frac{1}{3}\left(1-\frac{1}{\overline{R}_{0,1th}}\right)^2\right]-a. \tag{21}$$

After using Eqs. (14) and (20), Eq. (11) reduces R_{1th} into a function of H_1/L_1 and $\overline{R}_{0,1th}$

$$R_{1th}=\frac{(T_m-T_0)_{1th}}{q'''\pi R_0^2/k_f}=\frac{1}{\overline{R}_{0,1th}^2}\left\{\frac{(H_1/L_1)^2}{2\pi}+\frac{2}{3\pi k\varphi_{1,con}}\right\}+\frac{1}{\pi k\varphi_{1,con}}\times\frac{\overline{R}_{0,1th}-1}{(\varphi/\varphi_{1,con})\overline{R}_{0,1th}-1}\left(1-\frac{1}{\overline{R}_{0,1th}}\right)\left[1-\frac{1}{3}\left(1-\frac{1}{\overline{R}_{0,1th}}\right)^2\right]. \tag{22}$$

Our constructal design is thus reduced into the minimization of R_{1th} with respect to $\overline{R}_{0,1th}$. This minimization is normally desirable for two cases from the practical application point of view: (i) given H_1/L_1, and (ii) given the total number of slabs N_1 in periphery sectors defined by

$$N_1=\frac{2\pi R_0}{2H_1}=\frac{\pi\overline{R}_{0,1th}}{H_1/L_1}. \tag{23}$$

2.2.1. Minimize R_{1th} with respect to $\overline{R}_{0,1th}$ for given H_1/L_1

There are two means to resolve Eq. (17) for obtaining the constructal $\overline{R}_{0,1th}$. The first method (iteration method) is to solve the implicit equation, by iteration,

$$\begin{aligned}\frac{\partial R_{1th}}{\partial\overline{R}_{0,1th}}=&-\frac{2}{\overline{R}_{0,1th}^3}\left[\frac{(H_1/L_1)^2}{2\pi}+\frac{2}{3\pi k\varphi\tilde{\varphi}_{1,con}}\right]\\&+\frac{1}{3\pi k\varphi a\sqrt{1+\frac{A_1}{a}}}\left(\frac{1}{\overline{R}_{0,1th}}-\frac{2}{3\overline{R}_{0,1th}^3}+\frac{2a}{\overline{R}_{0,1th}^4}-\frac{8}{3\overline{R}_{0,1th}^4}\right.\\&\left.+\frac{6}{\overline{R}_{0,1th}^5}-\frac{16}{3\overline{R}_{0,1th}^6}+\frac{5}{3\overline{R}_{0,1th}^7}\right)+\frac{1}{\pi k\varphi(\overline{R}_{0,1th}-\tilde{\varphi}_{1,con})^2}\\&\times\left[\frac{\tilde{\varphi}_{1,con}^2}{2a\sqrt{1+\frac{A_1}{a}}}\left(-2\overline{R}_{0,1th}^2+\frac{8\overline{R}_{0,1th}}{3}-\frac{1}{9}-\frac{8}{\overline{R}_{0,1th}}+\frac{14}{3\overline{R}_{0,1th}^2}\right.\right.\\&\left.+\frac{8}{9\overline{R}_{0,1th}^3}+\frac{4}{3\overline{R}_{0,1th}^4}-\frac{16}{3\overline{R}_{0,1th}^5}+\frac{41}{9\overline{R}_{0,1th}^6}-\frac{4}{3\overline{R}_{0,1th}^7}\right)\\&-\tilde{\varphi}_{1,con}\left(\frac{1}{\overline{R}_{0,1th}^4}-\frac{4}{\overline{R}_{0,1th}^3}+\frac{2}{\overline{R}_{0,1th}^2}+\frac{2}{3}\right)\\&\left.+\left(\frac{4}{3\overline{R}_{0,1th}^3}-\frac{4}{\overline{R}_{0,1th}^2}+\frac{2}{\overline{R}_{0,1th}}+\frac{4}{3}\right)\right]=0.\end{aligned} \tag{24}$$

The second method (function-evaluation method), numerically simpler than the first method, first uses Eq. (22) to evaluate R_{1th} at different $\overline{R}_{0,1th}$ and then searches for the constructal $\overline{R}_{0,1th}$ that gives the minimum R_{1th} value. For example, we can easily obtain the $R_{1th}\sim\overline{R}_{0,1th}$ relation in Fig. 3 by the second method at $H_1/L_1 = 0.1$ and $k\varphi = 32$ (for Cu–water nanofluids, $k = 385/0.6$; and thus we have $k\varphi = 32$ at $\varphi = 0.05$). R_{1th} reaches its minimum (0.00611) when $\overline{R}_{0,1th}\cong 3.26$ at which $\tilde{\varphi}_{1,con}=0.584$ [Eq. (20)], $\widetilde{D}_{0,1th,con}=2.03$ [Eq. (14)] and $N_{1,con}$ = 103[Eq. (23)]. For zero-branching architecture, the disc overall thermal resistance $R_{0th}\cong 0.00822$ at $H_0/L_0 = 0.1$, and tends to minimum value 0.00663 as $H_0/L_0\to 0$. Therefore, the one-branching constructal configuration is better than its zero-branching counterpart for this case. Another striking feature is that the one-branching constructal configuration is independent of n_1. Even when $n_1 = 1$ so that one-branching architecture reduces to zero-branching architecture, the overall thermal resistance is still R_{1th} because the constructal slab width is determined by $\widetilde{D}_{0,1th,con}=2.03$ and $\overline{R}_{0,1th}\cong 3.26$ and is thus not uniform over the whole slab.

Consistent with the slender-sector assumption, we made the one-branching constructal design for different values of H_1/L_1 from

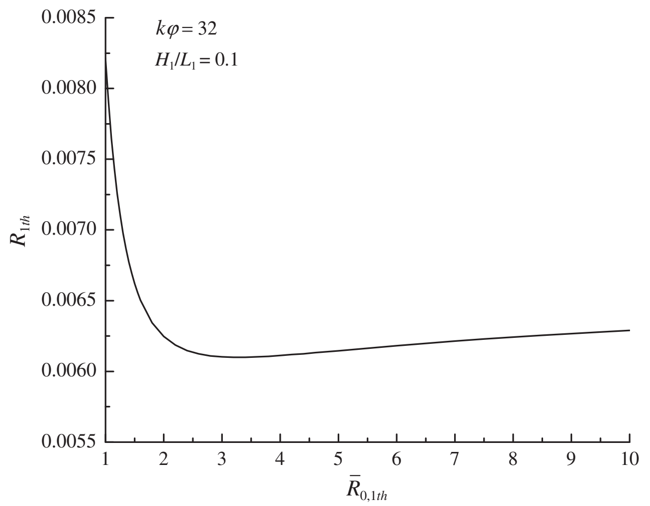

Fig. 3. Variation of overall thermal resistance R_{1th} with respect to $\bar{R}_{0,1th}$ in the one-branching architecture.

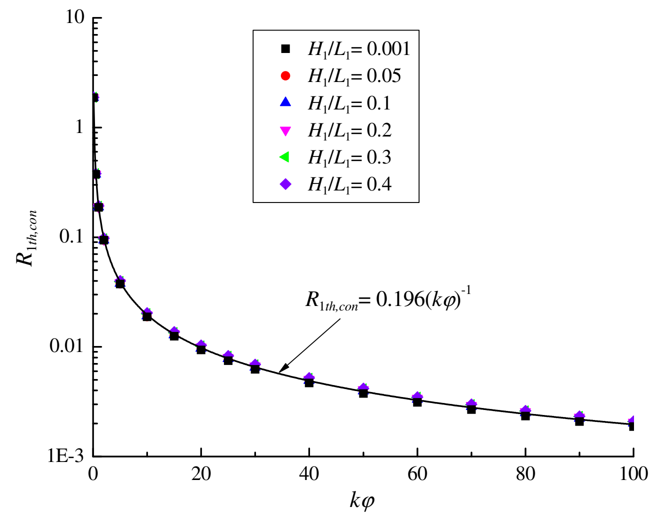

Fig. 5. Variation of $R_{1th,con}$ with $k\varphi$ and H_1/L_1 in one-branching architecture.

0 to 0.4. Fig. 4 shows the variation of $R_{1th,con}$, $\bar{R}_{0,1th,con}$, $\tilde{\varphi}_{1,con}$, $\tilde{D}_{0,1th,con}$ and $N_{1,con}$ with respect to H_1/L_1 at $k\varphi = 32$. R_{0th} [Eq. (3)] is also shown in Fig. 4 for comparing the zero- and one-branching architectures. Since $R_{1th,con}$ is always smaller than the minimum resistance of zero-branching architecture (0.00663 appearing at $H_0/L_0 = 0$), the one-branching configuration is desirable for reducing system overall thermal resistance. While R_{0th} increases significantly with the aspect ratio of periphery sectors [Eq. (3); Fig. 4], the H_1/L_1 sensitivity of $R_{1th,con}$ is very weak. Effects of $k\varphi$ and H_1/L_1 on $R_{1th,con}$ are shown in Fig. 5. Comparing with the $k\varphi$-effect, the effect of H_1/L_1 on $R_{1th,con}$ can be neglected. Actually, the data in Fig. 5 can be well represented by, with a relative error within 6% for $H_1/L_1 \in [0, 0.4]$,

$$R_{1th,con} = \frac{0.196}{k\varphi}. \tag{25}$$

Variation of $\bar{R}_{0,1th,con}$ with $k\varphi$ and H_1/L_1 is shown in Fig. 6. $\bar{R}_{0,1th,con}$ increases almost linearly with $k\varphi$. Its slope increases sensitively with H_1/L_1.

2.2.2. Minimize R_{1th} with respect to $\bar{R}_{0,1th}$ for given N_1

Note that $(H_1/L_1)^2/(2\pi\bar{R}^2_{0,1th}) = \pi/(2N_1^2)$ in Eqs. (11) and (22). With N_1 as a priori known, Eq. (17) reduces into

$$\frac{\partial R_{1th}}{\partial \bar{R}_{0,1th}} = \frac{1}{\pi k\varphi}\frac{\partial}{\partial \bar{R}_{0,1th}}\left\{\frac{2}{3\bar{R}^2_{0,1th}\tilde{\varphi}_{1,con}} + \frac{\bar{R}_{0,1th}-1}{\bar{R}_{0,1th}-\tilde{\varphi}_{1,con}}\left(1-\frac{1}{\bar{R}_{0,1th}}\right)\right.$$
$$\left.\times\left[1-\frac{1}{3}\left(1-\frac{1}{\bar{R}_{0,1th}}\right)^2\right]\right\} = 0. \tag{26}$$

Using Eq. (20) for $\tilde{\varphi}_{1,con} \sim \bar{R}_{0,1th}$ relation, solving Eq. (26) by the function-evaluation method yields the constructal configuration and system thermal resistance

$$\bar{R}_{0,1th,con} = 1.95, \tag{27}$$
$$\tilde{\varphi}_{1,con} = 0.762, \tag{28}$$
$$R_{1th,con} = \frac{\pi}{2N_1^2} + \frac{0.589}{\pi k\varphi}. \tag{29}$$

Therefore, the constructal configuration (both $\bar{R}_{0,1th,con}$ and $\tilde{\varphi}_{1,con}$) is independent of $k\varphi$ and N_1. When N_1 approaches to infinity so that H_1/L_1 tends to 0, R_{1th} has its minimum value $[0.589/(\pi k\varphi)]$.

The thermal resistance of zero-branching architecture [Eq. (3)] can be expressed as $\pi/(2N_0^2) + 2/(3\pi k\varphi)$, in which N_0 $[=2\pi R_0/(2H_0)]$ is the total number of slabs. For the same number of slabs

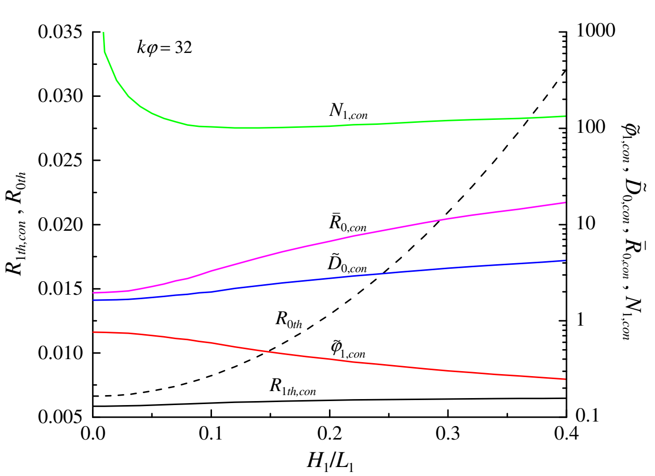

Fig. 4. Effect of aspect ratio H_1/L_1 on constructal configuration and system thermal resistance of one-branching architecture.

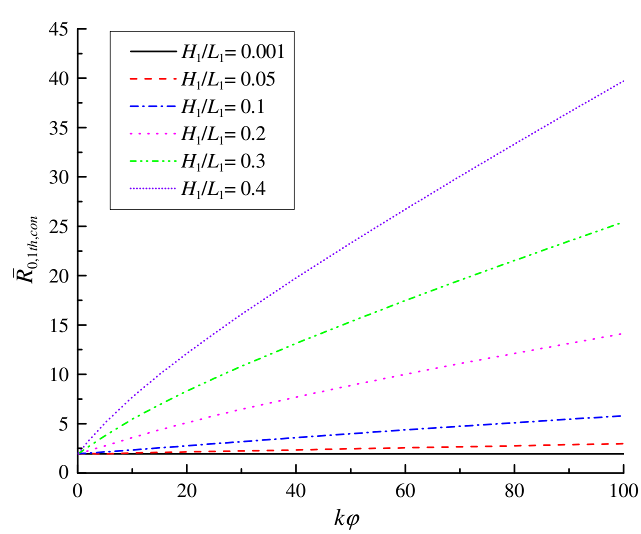

Fig. 6. Variation of $\bar{R}_{0,1th,con}$ with $k\varphi$ and H_1/L_1 in one-branching architecture.

in the periphery sectors (all slabs in zero-branching architecture are in the periphery sectors), we have

$$R_{0th} - R_{1th,con} \cong \frac{0.025}{k\varphi} \geqslant 0. \tag{30}$$

Therefore, the one-branching constructal structure always offers smaller system thermal resistance than the zero-branching configuration with the same number of slabs in the periphery sectors. The difference between the two becomes, however, insignificant as $k\varphi$ increases. The constructal R_{1th} is smaller than the minimum resistance of zero-branching architecture [$2/(3\pi k\varphi)$; appearing at $N_0 \to \infty$] when

$$N_1 > 7.97\sqrt{k\varphi}. \tag{31}$$

2.3. Two-branching architecture

Two-branching architecture consists of slabs that stretch radially to the distance L_0 away from the central heat sink, continue with n_1 branches that stretch radially to the distance of L_1, and further extends reach the rim with n_2 branches [Fig. 1(c)]. Its elemental sector, as shown in Fig. 2(c), contains one stem of aspect ratio H_0/L_0, n_1 tributaries of aspect ratio H_1/L_1, and n_1n_2 tributaries of aspect ratio H_2/L_2. L_0, L_1 and L_2 are the slab lengths in central sectors (Level-0 sectors), middle sectors (Level-1 sectors), and periphery sectors (Level-2 sectors), respectively. They also represent the distances from the central heat sink (T_0) to the confluence point of the n_1 branches in Level-1 sectors (T_{c1}), from the confluence point (T_{c1}) to the confluence point of the n_2 branches in Level-2 sectors (T_{c2}), and from the point (T_{c2}) to the hot spot (T_m), respectively. The goal is to assemble a number of branched sectors into the complete disc for a minimum overall thermal resistance R_{2th}.

By applying the results for one-branching architecture [Eq. (10)], $(T_m - T_{c1})$ can be calculated by

$$\begin{aligned}(T_m - T_{c1})_{2th} &= (T_m - T_{c2}) + (T_{c2} - T_{c1}) \\ &= \frac{q'''H_2L_2}{k_f}\left(\frac{1}{2}\frac{H_2}{L_2} + \frac{2}{3k\varphi_2}\frac{L_2}{H_2}\right) \\ &\quad + \frac{q'''L_1}{k_pD_1}\left[\frac{2}{3}H_1L_1 + \frac{n_2H_2}{R_1}(R_1^2 - L_1^2)\right].\end{aligned} \tag{32}$$

Here φ_2 is the slab volume fraction in Level-2 sectors. R_1 is the distance from the confluence point of Level-1 slabs to the rim, so that $R_1 = L_1 + L_2$.

The T_{c1} tip receives the heat which equals to the heat generation in the area between the arc with radius L_0 and the outer peripheral circumference. Following a similar analysis as that for one-branching architecture, we obtain

$$(T_{c1} - T_0)_{2th} = \frac{q'''L_0}{k_pD_0}\left[\frac{2}{3}H_0L_0 + \frac{n_1n_2H_2}{R_0}(R_0^2 - L_0^2)\right]. \tag{33}$$

Therefore, by adding Eqs. (32) and (33),

$$\begin{aligned}(T_m - T_0)_{2th} &= \frac{q'''H_2L_2}{k_f}\left(\frac{1}{2}\frac{H_2}{L_2} + \frac{2}{3k\varphi_2}\frac{L_2}{H_2}\right) \\ &\quad + \frac{q'''L_1}{k_pD_1}\left[\frac{2}{3}H_1L_1 + \frac{n_2H_2}{R_1}(R_1^2 - L_1^2)\right] \\ &\quad + \frac{q'''L_0}{k_pD_0}\left[\frac{2}{3}H_0L_0 + \frac{n_1n_2H_2}{R_0}(R_0^2 - L_0^2)\right].\end{aligned} \tag{34}$$

The disc overall thermal resistance R_{2th} is thus

$$\begin{aligned}R_{2th} &= \frac{(T_m - T_0)_{2th}}{q'''\pi R_0^2/k_f} \\ &= \frac{1}{\overline{R}_{0,2th}^2\overline{R}_{1,2th}^2}\left[\frac{(H_2/L_2)^2}{2\pi} + \frac{2}{3\pi k\varphi_2}\right] \\ &\quad + \frac{1}{\pi k\varphi_2}\frac{1}{\widetilde{D}_{1,2th}}\left(1 - \frac{1}{\overline{R}_{1,2th}}\right)\left[1 - \frac{1}{3}\left(1 - \frac{1}{\overline{R}_{1,2th}}\right)^2\right] \\ &\quad + \frac{1}{\pi k\varphi_2}\frac{1}{\widetilde{D}_{0,2th}}\left(1 - \frac{1}{\overline{R}_{0,2th}}\right)\left[1 - \frac{1}{3}\left(1 - \frac{1}{\overline{R}_{0,2th}}\right)^2\right],\end{aligned} \tag{35}$$

where $\overline{R}_{0,2th}, \overline{R}_{1,2th}, \widetilde{D}_{0,2th}$, and $\widetilde{D}_{1,2th}$ are defined by

$$\overline{R}_{0,2th} = \frac{R_0}{R_1}, \quad \overline{R}_{1,2th} = \frac{R_1}{L_2}, \quad \widetilde{D}_{0,2th} = \frac{D_0}{n_1n_2D_2}, \quad \widetilde{D}_{1,2th} = \frac{D_1}{n_2D_2}. \tag{36}$$

Here D_0, D_1 and D_2 are the slab widths in Level-0, Level-1 and Level-2 sectors, respectively [Fig. 2(c)].

Define $\varphi_{1\sim2}$ as the average slab volume fraction in all Level-1 and Level-2 sectors

$$\varphi_{1\sim2} = \frac{n_2D_2L_2 + D_1L_1}{n_2H_2R_1}, \tag{37}$$

so that $\widetilde{D}_{1,2th}$ can be written as

$$\widetilde{D}_{1,2th} = \frac{(\varphi_{1\sim2}/\varphi_2)\overline{R}_{1,2th} - 1}{\overline{R}_{1,2th} - 1}, \quad \varphi_2 < \varphi_{1\sim2}\overline{R}_{1,2th}. \tag{38}$$

Also,

$$\varphi = \frac{D_0L_0 + n_1D_1L_1 + n_1n_2D_2L_2}{n_1n_2H_2R_0}. \tag{39}$$

Therefore we can express $\varphi_2\widetilde{D}_{0,2th}$ in Eq. (35) by using $\varphi_{1\sim2}$, φ and $\overline{R}_{0,2th}$

$$\varphi_2\widetilde{D}_{0,2th} = \frac{\varphi\overline{R}_{0,2th} - \varphi_{1\sim2}}{\overline{R}_{0,2th} - 1}. \tag{40}$$

Substituting Eqs. (38) and (40) into Eq. (35) yields

$$\begin{aligned}R_{2th} = \frac{1}{\overline{R}_{0,2th}^2}&\left\{\frac{1}{\overline{R}_{1,2th}^2}\left[\frac{(H_2/L_2)^2}{2\pi} + \frac{2}{3\pi k\varphi_2}\right] + \frac{1}{\pi k\varphi_2}\frac{\overline{R}_{1,2th} - 1}{(\varphi_{1\sim2}/\varphi_2)\overline{R}_{1,2th} - 1}\left(1 - \frac{1}{\overline{R}_{1,2th}}\right)\right. \\ &\left.\times\left[1 - \frac{1}{3}\left(1 - \frac{1}{\overline{R}_{1,2th}}\right)^2\right]\right\} + \frac{1}{\pi k\varphi_{1\sim2}}\frac{\overline{R}_{0,2th} - 1}{(\varphi/\varphi_{1\sim2})\overline{R}_{0,2th} - 1} \\ &\times\left(1 - \frac{1}{\overline{R}_{0,2th}}\right)\left[1 - \frac{1}{3}\left(1 - \frac{1}{\overline{R}_{0,2th}}\right)^2\right].\end{aligned} \tag{41}$$

The term in the braces {} is the same as the one obtained by replacing $\overline{R}_{0,1th}$, H_1/L_1, φ_1 and φ in R_{1th} with $\overline{R}_{1,2th}$, H_2/L_2, φ_2 and $\varphi_{1\sim2}$, respectively. Moreover, $\overline{R}_{1,2th}$, H_2/L_2 and φ_2 appear only in the term in the braces {}. Hence the $\overline{R}_{0,1th,con}$ in Fig. 6 and the $\tilde{\varphi}_{1,con}$ in Eq. (20) can be directly applied to obtain the constructal $\overline{R}_{1,2th,con}$ and $\tilde{\varphi}_{2,con}$ simply replacing H_1/L_1 and φ with H_2/L_2 and $\varphi_{1\sim2}$. After applying the constructal $\overline{R}_{1,2th}$ and φ_2, the overall resistance R_{2th} is a function of (H_2/L_2, $\varphi_{1\sim2}$, $\overline{R}_{0,2th}$). As

$$\frac{\partial R_{2th}}{\partial(H_2/L_2)} = \frac{H_2/L_2}{\pi\overline{R}_{0,2th}^2\overline{R}_{1,2th}^2} \geqslant 0, \tag{42}$$

R_{2th} is a monotonic function of H_2/L_2. Therefore, our constructal design reduces into the minimization of R_{2th} with respect to $\varphi_{1\sim2}$ and $\overline{R}_{0,2th}$ under either given H_2/L_2 or given number N_2 of slabs in all periphery sectors defined by

$$N_2 = \frac{2\pi R_0}{2H_2} = \frac{\pi\overline{R}_{0,2th}\overline{R}_{1,2th}}{H_2/L_2}. \tag{43}$$

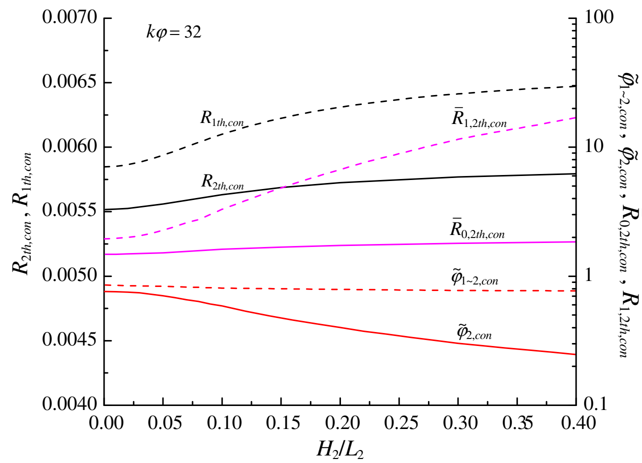

Fig. 7. Effect of aspect ratio H_2/L_2 on constructal configuration and system thermal resistance of two-branching architecture.

2.3.1. Minimize R_{2th} for given H_2/L_2

Based on Eq. (41), we made the constructal design (the minimization of R_{2th} with respect to $\varphi_{1\sim 2}$ and $\bar{R}_{0,2th}$) under specified H_2/L_2 from 0 to 0.4. Fig. 7 shows the variation of $R_{1th,con}$, $R_{2th,con}$, $\bar{R}_{0,2th,con}$, $\bar{R}_{1,2th,con}$, $\tilde{\varphi}_{2,con}$ and $\tilde{\varphi}_{1\sim 2,con}$ with respect to H_2/L_2 at $k\varphi = 32$. It shows that variations of $\bar{R}_{0,2th,con}$ and $\tilde{\varphi}_{1\sim 2,con}$ are very small in $H_2/L_2 \in [0, 0.4]$. The relative variation of $R_{2th,con}$ is less than 5% with H_2/L_2 changing from 0 to 0.4. $R_{2th,con}$ is 5–10% smaller than $R_{1th,con}$ for every value of H_2/L_2 (H_1/L_1 for $R_{1th,con}$) less than 0.4, and is always smaller than the minimum value of $R_{1th,con}$ [0.00586 at $H_1/L_1 \to 0$ or $N_1 \to \infty$; Eq. (29)].

If we neglect the weak effect of H_2/L_2 and H_1/L_1, we can approximate the term in the braces {} in Eq. (41) by $0.196/(k\varphi_{1\sim 2})$ [Fig. 5 and Eq. (25)] so that

$$R_{2th} = \frac{1}{\bar{R}^2_{0,2th}}\frac{0.196}{k\varphi_{1\sim 2}} + \frac{1}{\pi k\varphi_{1\sim 2}}\frac{\bar{R}_{0,2th}-1}{(\varphi/\varphi_{1\sim 2})\bar{R}_{0,2th}-1}\left(1-\frac{1}{\bar{R}_{0,2th}}\right)\left[1-\frac{1}{3}\left(1-\frac{1}{\bar{R}_{0,2th}}\right)^2\right]. \tag{44}$$

The minimization of R_{2th} with respect to $\varphi_{1\sim 2}$ requires

$$\frac{\partial R_{2th}}{\partial \varphi_{1\sim 2}} = \frac{1}{\pi k}\frac{\partial}{\partial \varphi_{1\sim 2}}\left\{\frac{0.196\pi}{\bar{R}^2_{0,2th}\varphi_{1\sim 2}} + \frac{\bar{R}_{0,2th}-1}{\varphi\bar{R}_{0,2th}-\varphi_{1\sim 2}}\left(1-\frac{1}{\bar{R}_{0,2th}}\right)\times\left[1-\frac{1}{3}\left(1-\frac{1}{\bar{R}_{0,2th}}\right)^2\right]\right\} = 0. \tag{45}$$

Its solution is readily obtained by Eqs. (19)–(21),

$$\tilde{\varphi}_{1\sim 2,con} = \varphi_{1\sim 2,con}/\varphi = \frac{0.196\pi\bar{R}_{0,2th}}{A_{21}}\left(\sqrt{1+\frac{A_{21}}{0.196\pi}}-1\right), \tag{46}$$

where

$$A_{21} = (\bar{R}_{0,2th}-1)\left(1-\frac{1}{\bar{R}_{0,2th}}\right)\left[\bar{R}^2_{0,2th}-\frac{1}{3}\left(1-\frac{1}{\bar{R}_{0,2th}}\right)^2\right] - 0.196\pi. \tag{47}$$

After substituting Eq. (46) into Eq. (44), the minimization of R_{2th} with respect to $\bar{R}_{0,2th}$ becomes resolving

$$\frac{\partial R_{2th}}{\partial \bar{R}_{0,2th}} = \frac{1}{\pi k\varphi}\frac{\partial}{\partial \bar{R}_{0,2th}}\left\{\frac{0.196\pi}{\bar{R}^2_{0,2th}\tilde{\varphi}_{1\sim 2,con}} + \frac{\bar{R}_{0,2th}-1}{\bar{R}_{0,2th}-\tilde{\varphi}_{1\sim 2,con}}\left(1-\frac{1}{\bar{R}_{0,2th}}\right)\times\left[1-\frac{1}{3}\left(1-\frac{1}{\bar{R}_{0,2th}}\right)^2\right]\right\} = 0. \tag{48}$$

Its solution is, by the function-evaluation method,

$$\bar{R}_{0,2th,con} = 1.62, \tag{49}$$

$$\tilde{\varphi}_{1\sim 2,con} = 0.819, \tag{50}$$

$$R_{2th,con} = \frac{0.568}{\pi k\varphi}. \tag{51}$$

Therefore, the constructal configuration (both $\bar{R}_{0,2th,con}$ and $\tilde{\varphi}_{1\sim 2,con}$) is independent of $k\varphi$ and H_2/L_2. The invariance of the constructal configuration with H_2/L_2 come from the negligible effect of H_2/L_2 on the overall resistance. Like $R_{1th,con}$, $R_{2th,con}$ is also inversely proportional to $k\varphi$. Also,

$$\frac{R_{2th,con}}{R_{1th,con}} \cong 0.92. \tag{52}$$

Therefore, we can reduce the system resistance by 8% by shifting the configuration from one- to two-branching structure.

A comparison of $R_{2th,con}$in Eq. (51) with its exact value shows that Eq. (51) is accurate within 2.5%. Note also that the accuracy of Eq. (25) is 6%. Therefore, the effect of the aspect ratio on the constructal overall thermal resistance will become weaker and weaker as the branching level increases.

2.3.2. Minimize R_{2th} for given N_2

Note that in Eq. (41) $(H_2/L_2)^2/(2\pi\bar{R}^2_{0,2th}\bar{R}^2_{1,2th}) = \pi/(2N_2^2)$ by using Eq. (43). R_{2th} reduces to

$$R_{2th} = \frac{\pi}{2N_2^2} + \frac{1}{\bar{R}^2_{0,2th}}\left\{\frac{1}{\bar{R}^2_{1,2th}}\frac{2}{3\pi k\varphi_2} + \frac{1}{\pi k\varphi_2}\frac{\bar{R}_{1,2th}-1}{(\varphi_{1\sim 2}/\varphi_2)\bar{R}_{1,2th}-1}\left(1-\frac{1}{\bar{R}_{1,2th}}\right)\times\left[1-\frac{1}{3}\left(1-\frac{1}{\bar{R}_{1,2th}}\right)^2\right]\right\} + \frac{1}{\pi k\varphi_{1\sim 2}}\frac{\bar{R}_{0,2th}-1}{(\varphi/\varphi_{1\sim 2})\bar{R}_{0,2th}-1}\left(1-\frac{1}{\bar{R}_{0,2th}}\right)\times\left[1-\frac{1}{3}\left(1-\frac{1}{\bar{R}_{0,2th}}\right)^2\right]. \tag{53}$$

According to the result for the one-branching architecture, the term in the braces {} has its minimum value [$0.589/(\pi k\varphi_{1\sim 2})$, Eq. (29)] when $\bar{R}_{1,2th} = 1.95$ [Eq. (27)]. By replacing the term in the braces {} with [$0.589/(\pi k\varphi_{1\sim 2})$] in Eq. (53), Eq. (53) becomes

$$R_{2th} = \frac{\pi}{2N_2^2} + \frac{1}{\pi k\varphi}\left\{\frac{0.589}{\bar{R}^2_{0,2th}\tilde{\varphi}_{1\sim 2}} + \frac{\bar{R}_{0,2th}-1}{\bar{R}_{0,2th}-\tilde{\varphi}_{1\sim 2}}\left(1-\frac{1}{\bar{R}_{0,2th}}\right)\times\left[1-\frac{1}{3}\left(1-\frac{1}{\bar{R}_{0,2th}}\right)^2\right]\right\}. \tag{54}$$

The minimization of R_{2th} with respect to $\varphi_{1\sim 2}$ requires

$$\frac{\partial R_{2th}}{\partial \tilde{\varphi}_{1\sim 2}} = \frac{1}{\pi k}\frac{\partial}{\partial \varphi_{1\sim 2}}\left\{\frac{0.589}{\bar{R}^2_{0,2th}\varphi_{1\sim 2}} + \frac{\bar{R}_{0,2th}-1}{\varphi\bar{R}_{0,2th}-\varphi_{1\sim 2}}\left(1-\frac{1}{\bar{R}_{0,2th}}\right)\times\left[1-\frac{1}{3}\left(1-\frac{1}{\bar{R}_{0,2th}}\right)^2\right]\right\} = 0. \tag{55}$$

Its solution reads, by Eq. (19)–(21),

$$\tilde{\varphi}_{1\sim 2,con} = \frac{\varphi_{1\sim 2,con}}{\varphi} = \frac{0.589\bar{R}_{0,2th}}{A_{22}}\left(\sqrt{1+\frac{A_{22}}{0.589}}-1\right), \tag{56}$$

where

$$A_{22} = (\overline{R}_{0,2th} - 1)\left(1 - \frac{1}{\overline{R}_{0,2th}}\right)\left[\overline{R}^2_{0,2th} - \frac{1}{3}\left(1 - \frac{1}{\overline{R}_{0,2th}}\right)^2\right] - 0.589. \tag{57}$$

After substituting Eq. (56) into Eq. (54), the minimization of R_{2th} with respect to $\overline{R}_{0,2th}$ reduces into resolving,

$$\frac{\partial R_{2th}}{\partial \overline{R}_{0,2th}} = \frac{1}{\pi k\varphi}\frac{\partial}{\partial \overline{R}_{0,2th}}\left\{\frac{0.589}{\overline{R}^2_{0,2th}\tilde{\varphi}_{1\sim2,con}} + \frac{\overline{R}_{0,2th} - 1}{\overline{R}_{0,2th} - \tilde{\varphi}_{1\sim2,con}}\left(1 - \frac{1}{\overline{R}_{0,2th}}\right)\times\left[1 - \frac{1}{3}\left(1 - \frac{1}{\overline{R}_{0,2th}}\right)^2\right]\right\} = 0. \tag{58}$$

Its solution is readily available by using the function-evaluation method,

$$\overline{R}_{0,2th,con} = 1.48, \tag{59}$$

$$\tilde{\varphi}_{1\sim2,con} = 0.848, \tag{60}$$

$$R_{2th,con} = \frac{\pi}{2N_2^2} + \frac{0.555/\pi}{k\varphi}. \tag{61}$$

For the same number of slabs in the periphery sectors, Eqs. (29) and (61) yields

$$R_{1th,con} - R_{2th,con} \cong \frac{0.011}{k\varphi} \geqslant 0. \tag{62}$$

Therefore, the two-branching constructal structure always offers smaller system overall thermal resistance than the one-branching configuration with the same number of slabs in the periphery sectors. The difference between the two becomes insignificant as $k\varphi$ increases. The constructal R_{2th} is also smaller than the minimum $R_{1th,con}$ [$0.589/(\pi k\varphi)$, Eq. (29)] when

$$N_2 > 12.05\sqrt{k\varphi}. \tag{63}$$

2.4. M-branching architecture

Our constructal design can be made up to M-branching architecture in which the sectors from the center to rim are named in sequence as Level-0, Level-1, Level-2, until Level-M sectors. Here M can be any natural number. The system overall temperature difference $(T_m - T_0)_{Mth}$ is the sum of $(T_m - T_{c1})_{Mth}$ and $(T_{c1} - T_0)_{Mth}$, in which $(T_m - T_{c1})_{Mth}$ is available from the $(M-1)$-branching analysis, simply renumbering the parameters from Level-0 to Level-$(M-1)$ with the corresponding parameters from Level-1 to Level-M. Define the relative radius

$$\overline{R}_i = \frac{R_i}{R_{i+1}} \quad (i = 0, 1, \ldots, M-1), \tag{64}$$

where R_i is the distance from the confluence point of the slabs in Level-i sectors to the rim such that

$$R_i = \sum_{j=i}^{M} L_j \quad (i = 0, 1, \ldots, M), \tag{65}$$

with L_j being the length of slabs in Level-j sectors. The system overall thermal resistance R_{Mth} can thus be written as

$$\begin{aligned} R_{Mth} &= \frac{(T_m - T_0)_{Mth}}{q'''\pi R_0^2/k_f} = \frac{(T_m - T_{c1})_{Mth} - (T_{c1} - T_0)_{Mth}}{q'''\pi R_0^2/k_f} \\ &= \frac{1}{\overline{R}^2_{0,Mth}}\{R_{(M-1)th}\} + \frac{1}{\pi k\varphi_{1\sim M}} \\ &\quad\times\frac{\overline{R}_{0,Mth} - 1}{(\varphi/\varphi_{1\sim M})\overline{R}_{0,Mth} - 1}\left(1 - \frac{1}{\overline{R}_{0,Mth}}\right)\left[1 - \frac{1}{3}\left(1 - \frac{1}{\overline{R}_{0,Mth}}\right)^2\right]. \end{aligned} \tag{66}$$

Here $R_{(M-1)th}$ is the overall resistance for $(M-1)$-branching architecture in which the parameters in Level-i replaced by the parameters in Level-$(i+1)$ with i ranging from 0 to $(M-1)$. $\varphi_{1\sim M}$ denotes the slab volume fraction in all sectors from Level-1 to Level-M.

Define the non-dimensional slab width

$$\widetilde{D}_i = \frac{D_i}{D_M\prod_{j=i+1}^{M} n_j} \quad (i = 0, 1, \ldots, M-1), \tag{67}$$

where D_i is the slab width in Level-i sectors, and n_j is the number of branches bifurcated from one slab in Level-$(j-1)$ sectors. R_{Mth} becomes

$$R_{Mth} = \frac{1}{\prod_{i=0}^{M-1}\overline{R}_i^2}\left[\frac{(H_M/L_M)^2}{2\pi} + \frac{2}{3\pi k\varphi_M}\right] + \frac{1}{\pi k\varphi_M}\sum_{i=0}^{M-1}\frac{1}{\widetilde{D}_i}\times\frac{1}{\prod_{j=0}^{i-1}\overline{R}_j^2}\left(1 - \frac{1}{\overline{R}_i}\right)\left[1 - \frac{1}{3}\left(1 - \frac{1}{\overline{R}_i}\right)^2\right]. \tag{68}$$

We can then perform our constructal design by recursion up to the M-branching architecture to find its constructal configuration for minimized overall thermal resistance. The configurational parameters to be determined include: the relative radius $\overline{R}_i$ and slab volume fraction $\varphi_{(i+1)\sim M}$ for $i = 0, 1, \ldots, M-1$, with either the aspect ratio of the periphery sectors (Level-M sectors, H_M/L_M) or the total number of slabs in the periphery sectors (N_M) as a given restriction, from which the slab width in each level ($\widetilde{D}_i, i = 0, 1, \ldots, M-1$) and the aspect ratio of sectors of other levels (H_i/L_i, $i = 0, 1, \ldots, M-1$) can be obtained. The striking feature of the overall thermal resistance is its invariance with the numbers of bifurcated slabs in all levels (n_i; $i = 1, 2, \ldots, M$).

2.4.1. Minimize R_{Mth} for given H_M/L_M

In a precise sense, the constructal geometry and corresponding constructal thermal resistance $R_{Mth,con}$ always depend on the value of H_M/L_M. However, the effect of H_M/L_M becomes weaker and weaker with M increasing. When $k\varphi = 32$, for example, $R_{0th,con}$, $R_{1th,con}$ and $R_{2th,con}$ increase by 384%, 11% and 5%, respectively, with H_0/L_0, H_1/L_1 or H_2/L_2 increasing from 0 to 0.4 (Figs. 4 and 7). The effect of H_2/L_2 on $\overline{R}_{0,2th,con}$ and $\tilde{\varphi}_{1\sim2,con}$ is much weaker than the effect of H_1/L_1 on $\overline{R}_{0,1th,con}$ and $\tilde{\varphi}_{1,con}$ (Fig. 7). Therefore we neglect this weak effect in designing the M-branching architecture. Following a similar procedure as that used to obtain Eqs. (49)–(51), we can rewrite the overall thermal resistance R_{Mth} as

$$\begin{aligned} R_{Mth} &= \frac{1}{\overline{R}^2_{0,Mth}}\{R_{(M-1)th}\} \\ &\quad + \frac{\overline{R}_{0,Mth} - 1}{\pi k\varphi\overline{R}_{0,Mth} - \pi k\varphi_{1\sim M,con}}\left(1 - \frac{1}{\overline{R}_{0,Mth}}\right)\left[1 - \frac{1}{3}\left(1 - \frac{1}{\overline{R}_{0,Mth}}\right)^2\right] \\ &= \frac{a_{(M-1)1}}{\pi k\varphi_{1\sim M}\overline{R}^2_{0,Mth}} \\ &\quad + \frac{\overline{R}_{0,Mth} - 1}{\pi k\varphi\overline{R}_{0,Mth} - \pi k\varphi_{1\sim M,con}}\left(1 - \frac{1}{\overline{R}_{0,Mth}}\right)\left[1 - \frac{1}{3}\left(1 - \frac{1}{\overline{R}_{0,Mth}}\right)^2\right]. \end{aligned} \tag{69}$$

Here $a_{(M-1)1}$ is the constant appearing in $R_{(M-1)th,con}$, and a_{21} has been shown to be 0.568. The minimization of R_{Mth} with respect to $\varphi_{1\sim M,con}$ requires

$$\frac{\partial R_{Mth}}{\partial \varphi_{1\sim M,con}} = \frac{1}{\pi k}\frac{\partial}{\partial \varphi_{1\sim M,con}}\left\{\frac{a_{(M-1)1}}{\overline{R}^2_{0,Mth}\varphi_{1\sim M,con}} + \frac{\overline{R}_{0,Mth} - 1}{\varphi\overline{R}_{0,Mth} - \varphi_{1\sim M,con}}\times\left(1 - \frac{1}{\overline{R}_{0,Mth}}\right)\left[1 - \frac{1}{3}\left(1 - \frac{1}{\overline{R}_{0,Mth}}\right)^2\right]\right\} = 0. \tag{70}$$

Its solution is, by Eq. (19)–(21),

$$\tilde{\varphi}_{1\sim M,con} = \varphi_{1\sim M,con}/\varphi = \frac{a_{(M-1)1}\overline{R}_{0,Mth}}{A_{M1}}\left(\sqrt{1+\frac{A_{M1}}{a_{(M-1)1}}}-1\right), \tag{71}$$

where

$$A_{M1} = (\overline{R}_{0,Mth}-1)\left(1-\frac{1}{\overline{R}_{0,Mth}}\right)\left[\overline{R}_{0,Mth}^2-\frac{1}{3}\left(1-\frac{1}{\overline{R}_{0,Mth}}\right)^2\right]-a_{(M-1)1}. \tag{72}$$

After substituting Eq. (71) into Eq. (69), we can minimize R_{Mth} with respect to $\overline{R}_{0,Mth}$ by resolving

$$\frac{\partial R_{Mth}}{\partial \overline{R}_{0,Mth}} = \frac{1}{\pi k\varphi}\frac{\partial}{\partial \overline{R}_{0,Mth}}\left\{\frac{a_{(M-1)1}}{\overline{R}_{0,Mth}^2\tilde{\varphi}_{1\sim M,con}}+\frac{\overline{R}_{0,Mth}-1}{\overline{R}_{0,Mth}-\tilde{\varphi}_{1\sim M,con}}\times\left(1-\frac{1}{\overline{R}_{0,Mth}}\right)\left[1-\frac{1}{3}\left(1-\frac{1}{\overline{R}_{0,Mth}}\right)^2\right]\right\}=0. \tag{73}$$

We then apply the function-evaluation method to obtain

$$R_{Mth,con} = \frac{a_{M1}}{\pi k\varphi}, \tag{74}$$

$$\overline{R}_{0,Mth,con} = b_{M1}, \tag{75}$$

$$\tilde{\varphi}_{1\sim M,con} = c_{M1}, \tag{76}$$

where a_{M1}, b_{M1} and c_{M1} are listed in Table 1. The constructal slab volume fraction increases from the periphery sectors to the central sectors (c_{M1} in Table 1). The constructal disc overall thermal resistance decreases with M increasing (a_{M1} in Table 1). However, the decreasing rate becomes smaller and smaller.

2.4.2. Minimize R_{Mth} for given N_M

Note that in Eq. (68)

$$\frac{(H_M/L_M)^2}{2\pi\prod_{i=0}^{M-1}\overline{R}_i^2} = \frac{\pi}{2N_M^2}. \tag{77}$$

Hence R_{2th} reduces into

$$R_{Mth} = \frac{\pi}{2N_M^2}+\frac{1}{\overline{R}_{0,Mth}^2}\left\{R_{(M-1)th}-\frac{\pi}{2N_{(M-1)}^2}\right\}+\frac{\overline{R}_{0,Mth}-1}{\pi k\varphi\overline{R}_{0,Mth}-\pi k\varphi_{1\sim M,con}}\left(1-\frac{1}{\overline{R}_{0,Mth}}\right)\left[1-\frac{1}{3}\left(1-\frac{1}{\overline{R}_{0,Mth}}\right)^2\right]. \tag{78}$$

The constructal $\varphi_{1\sim M,con}$ to minimize R_{Mth} can be obtained from

$$\frac{\partial R_{Mth}}{\partial \varphi_{1\sim M}} = \frac{\partial}{\partial \varphi_{1\sim M}}\left\{\frac{a_{(M-1)2}}{\overline{R}_{0,Mth}^2\varphi_{1\sim M}}+\frac{\overline{R}_{0,Mth}-1}{\varphi\overline{R}_{0,Mth}-\varphi_{1\sim M}}\left(1-\frac{1}{\overline{R}_{0,Mth}}\right)\times\left[1-\frac{1}{3}\left(1-\frac{1}{\overline{R}_{0,Mth}}\right)^2\right]\right\}=0. \tag{79}$$

Clearly, a_{12} and a_{22} are 0.589 and 0.555, respectively, as shown in Eqs. (29) and (61). The solution of Eq. (79) is, by Eq. (19)–(21),

$$\tilde{\varphi}_{1\sim M,con} = \varphi_{1\sim M,con}/\varphi = \frac{a_{(M-1)2}\overline{R}_{0,Mth}}{A_{M2}}\left(\sqrt{1+\frac{A_{M2}}{a_{(M-1)2}}}-1\right), \tag{80}$$

where

$$A_{M2} = (\overline{R}_{0,Mth}-1)\left(1-\frac{1}{\overline{R}_{0,Mth}}\right)\left[\overline{R}_{0,Mth}^2-\frac{1}{3}\left(1-\frac{1}{\overline{R}_{0,Mth}}\right)^2\right]-a_{(M-1)2}. \tag{81}$$

After substituting Eq. (80) into Eq. (78), the minimization of R_{Mth} with respect to $\overline{R}_{0,Mth}$ requires

$$\frac{\partial R_{Mth}}{\partial \overline{R}_{0,Mth}} = \frac{1}{\pi k\varphi}\frac{\partial}{\partial \overline{R}_{0,Mth}}\left\{\frac{a_{(M-1)2}}{\overline{R}_{0,Mth}^2\tilde{\varphi}_{1\sim M,con}}+\frac{\overline{R}_{0,Mth}-1}{\overline{R}_{0,Mth}-\tilde{\varphi}_{1\sim M,con}}\left(-\frac{1}{\overline{R}_{0,Mth}}\right)\times\left[1-\frac{1}{3}\left(1-\frac{1}{\overline{R}_{0,Mth}}\right)^2\right]\right\}=0. \tag{82}$$

We then apply the function-evaluation method to obtain

$$R_{Mth,con} = \frac{\pi}{2N_M^2}+\frac{a_{M2}}{\pi k\varphi}, \tag{83}$$

$$\overline{R}_{0,Mth,con} = b_{M2}, \tag{84}$$

$$\tilde{\varphi}_{1\sim M,con} = c_{M2}, \tag{85}$$

where a_{M2}, b_{M2} and c_{M2} are also listed in Table 1. The constructal geometry of M-branching architecture has approximately the same slab length in every level (b_{M2} in Table 1). The constructal slab volume fraction decreases from Level-0 to Level-M sectors (c_{M2} in Table 1). With the increase of branching level M, the constructal overall thermal resistance decreases with the rate of decreasing becoming smaller and smaller (a_{M2} in Table 1). Note also that $\overline{R}_{i,Mth,con}$ and $\tilde{\varphi}_{(i+1)\sim M,con}$ for M-branching architecture are equivalent to $\overline{R}_{0,(M-i)th,con}$ and $\tilde{\varphi}_{1\sim(M-i),con}$ for $(M-i)$-branching architecture.

Our analysis of either specified aspect ratio or specified slab number in the periphery sectors shows that the constructal overall resistance can be reduced via using more branching configuration. This reduction is however not necessarily true in the other systems [15,16]. Note also that the constructal configuration and resistance are independent of the numbers of bifurcated slabs at any branching levels (n_i; $i = 1,2,\ldots,M$). In case of $n_i(i = 1,2,\ldots,M) = 1$, the constructal configuration reduces into the one like the zero-branching structure, but with the variation of the slab width from one level to another. The constructal slab width at i-level ($\widetilde{D}_{i,Mth,con}$) can be obtained by

$$\widetilde{D}_{i,Mth,con} = \frac{D_{i,Mth}}{D_{i+1,Mth}} = \frac{1}{\prod_{j=i+1}^{M-1}\tilde{\varphi}_{1\sim(M-j),con}}\frac{\tilde{\varphi}_{1\sim(M-i),con}\overline{R}_{0,(M-i)th}-1}{\overline{R}_{0,(M-i)th}-1}. \tag{86}$$

The constructal slab width thus increases from periphery sectors to central sectors (Table 1). This is consistent with the result in [13] that the optimal shape of the high-conductivity slab is the

Table 1
Constants in Eqs. (74)–(76) (specified aspect ratio in periphery sectors) and (83)–(85) (specified number of slabs in periphery sectors).

M	a_{M1}	b_{M1}	c_{M1}	a_{M2}	b_{M2}	c_{M2}
1	–	–	–	0.589	1.95	0.762
2	0.568	1.62	0.819	0.555	1.48	0.848
3	0.543	1.38	0.869	0.535	1.33	0.884
4	0.527	1.28	0.896	0.521	1.25	0.905
5	0.515	1.23	0.913	0.511	1.21	0.919
6	0.507	1.19	0.924	0.504	1.18	0.929
7	0.500	1.16	0.933	0.498	1.15	0.936
8	0.495	1.14	0.940	0.493	1.14	0.943
9	0.491	1.13	0.945	0.489	1.12	0.948
10	0.487	1.12	0.950	0.486	1.11	0.952
11	0.484	1.11	0.954	0.483	1.10	0.955
12	0.482	1.10	0.957	0.480	1.09	0.958

one with the thicker root at disc center and the blunt tip at disc rim (Fig. 2 in [13]).

3. Concluding remarks

Practical applications of nanofluids as the heat-conduction fluids often have an ultimate system aim such as minimization of system highest temperature and minimization of system overall thermal resistance. The microstructural optimization for the best system performance is however a very difficult, unresolved problem of inverse type. We have thus developed a constructal approach that is based on the constructal theory, converts the inverse problem into a forward one by first specifying a type of microstructures and then optimizing system performance with respect to the available freedom within the specified type of microstructures, and enables us to find the constructal microstructure (the best for the optimal system performance within the specified type of microstructures).

The constructal design of nanofluids with any branching level of tree-shaped nanoparticle configuration is made to cool a circular disc with uniform heat generation and a central heat sink. The obtained constructal structure provides the best distributions of relative lengths of sectors and particle volume fractions which minimize the system overall resistance with either the aspect ratio or the total number of periphery sectors as a priori known. The constructal slab length varies little from one level to another except the periphery sectors for given aspect ratio of the periphery sectors. The constructal particle volume fraction increases from peripheral to central sectors. The constructal configuration has some universal features of independent of: (i) numbers of bifurcated slabs at any branching levels, (ii) fluid and particle properties, and (iii) particle overall volume fraction.

The constructal system thermal resistance is inversely proportional to the product of particle–fluid conductivity ratio and particle overall volume fraction. The proportional coefficient is constant with its value decreasing as the branching level increases. Therefore, the constructal system resistance can be made smaller for fixed material properties and particle overall volume fraction by using more level of branching structure. With the prescribed total slab number in the periphery sectors, the constructal system resistance decreases as the slab number increases. With the prescribed aspect ratio of periphery sectors, the constructal system resistance decreases with decreasing aspect ratio. This dependency is however very weak except the zero-branching architecture and becomes even weaker as the branching level increases. Therefore this dependency can be practically neglected.

The constructal approach developed in the present work is also valid for other problems of inverse or downscaling type.

Acknowledgement

The financial support from the Research Grants Council of Hong Kong (GRF718009 and GRF717508) is gratefully acknowledged.

References

[1] S.U.S. Choi, Nanofluids: from vision to reality through research, ASME J. Heat Transfer 131 (2009) 033106.
[2] G.P. Peterson, C.H. Li, Heat and mass transfer in fluids with nanoparticle suspensions, Adv. Heat Transfer 39 (2006) 257–376.
[3] S.K. Das, S.U.S. Choi, W. Yu, T. Pradeep, Nanofluids: Science and Technology, John Wiley & Sons, Inc., Hoboken, New Jersey, 2008.
[4] P. Vadasz, Heat conduction in nanofluid suspensions, ASME J. Heat Transfer 128 (2006) 465–477.
[5] P. Vadasz, Nanofluid suspensions and bi-composite media as derivatives of interface heat transfer modeling in porous media, in: P. Vadasz (Ed.), Emerging Topics in Heat and Mass Transfer in Porous Media, Springer, Berlin, 2008, pp. 283–326.
[6] D.Y. Tzou, Thermal instability of nanofluids in natural convection, Int. J. Heat Mass Transfer 51 (2008) 2967–2979.
[7] S.J. Kim, T. McKrell, J. Buongiorno, L.W. Hu, Experimental study of flow critical heat flux in alumina–water, zinc-oxide–water, and diamond–water nanofluids, ASME J. Heat Transfer 131 (2009) 043204.
[8] L.Q. Wang, M. Quintard, Nanofluids of the Future, Advances in Transport Phenomena, Springer, Heidelberg, 2009. pp. 179–243.
[9] L.Q. Wang, M.T. Xu, X.H. Wei, Multiscale theorems, Adv. Chem. Eng. 34 (2008) 175–468.
[10] A. Bejan, S. Lorente, Design with Constructal Theory, Wiley, New Jersey, 2008.
[11] A.H. Reis, Constructal theory: from engineering to physics, and how flow systems develop shape and structure, App. Mech. Rev. 59 (2006) 269–282.
[12] A. Bejan, S. Lorente, Constructal theory of configuration generation in nature and engineering, J. Appl. Phys. 100 (2006) 041301.
[13] L.A.O. Rocha, S. Lorente, A. Bejan, Constructal design for cooling a disc-shaped area by conduction, Int. J. Heat Mass Transfer 45 (2002) 1643–1652.
[14] A. Bejan, N. Dan, Two constructal routes to minimal heat flow resistance via greater internal complexity, ASME J. Heat Transfer 121 (1999) 6–14.
[15] L. Kuddusi, N. Eğrican, A critical review of constructal theory, Energy Convers. Manage. 49 (2008) 1283–1294.
[16] L. Ghodoossi, Conceptual study on constructal theory, Energy Convers. Manage. 45 (2004) 1379–1395.